Proceedings of ICFDP7:
7TH Int. Congress on Fluid Dynamics & Propulsion
December 18-20, 2001, Cairo, Egypt

ICFDP7-2001017

PREDICTION OF WIND-FARM PEFORMANCE : CHALLENGES AND EXPECTATIONS

M.A.Serag-Eldin
American University in Cairo
P.O.box 2511, Cairo,Egypt.
Email:massd948@aucegypt.edu

ABSTRACT

The paper addresses the challenges met when attempting to predict Wind-farm performance . It first discusses the prediction problems, and then presents solutions to many of these problems referring to previously published work . The paper also presents a new computational model which employs cyclic-boundary conditions to predict the performance of very large wind-farms subject to wind inclined to the rows of turbines. The results are displayed and discussed.

INTRODUCTION

Wind farms are large-scale energy applications whose performance predictions offer a real challenge. The common wind-farm is designed to convert the instantaneous energy available in the wind into electrical energy output, the latter being fed into an electrical grid. Wind farms comprise a wide array of installed wind energy conversion systems, WECS, each unit employing horizontal axis wind turbines, HAWT.

The wind speed and direction are random variables which are site specific; the energy available in the wind is proportional to the cube of the wind speed, so that small fluctuations in wind speed result in wide fluctuations in available energy. Moreover, the electrical energy output is not a linear function of the wind energy input, but is a non-linear function which depends on the WECS characteristics. Indeed, WECS are designed to produce zero output below a certain cut-in speed and above a certain cut-out speed to protect the blades and the generator. Thus the electrical input to the network is also highly fluctuating.

Yet wind-farms are expensive enterprises, and the prediction of their performance is essential for undertaking a feasibility study. In view of the narrow economic margin it may display, every effort should be made to make this prediction as accurate as possible.

Performance prediction of wind farms is essential at the design stage of a new farm in order to select the best WECS characteristics and/or distribute the WECS spacing economically. The closer the spacing between the units the more the interference losses, but the smaller the area of the wind farm for a given number of units and the lower the installation, interconnection, operation and maintenance costs. It is usual for wind farm sites to display pre-dominant wind directions; in this case economic considerations dictate that the turbine units are staggered and distributed over rectangular arrays with longer spacing in the predominant direction. For sites displaying nearly omni-directional winds, it is reasonable to employ 15 turbine-diameter spacing in the predominant direction and only 5 turbine-diameter spacing in the cross-stream direction. However, this necessitates that performance prediction is conducted for each direction separately as the interference effect will be different for each direction.

Performance predictions may also be required after the erection of the wind farm in order to predict the effect of introducing additional turbine rows or to replace the current WECS units with newer ones of different characteristics. Since no two sites are identical, performance predictions need to be performed for each site independently.

Even if the free wind speed profile, direction and other characteristics were known at an appropriate distance upstream of the wind farm, the output of the wind farm corresponding to those known conditions is still not easily predicted. This is

mainly because each wind turbine output depends on the interaction between the local wind speed and the local WECS characteristics, and this effect is two way, i.e. the WECS affects the local wind by creating a wake and the local wind determines the WECS performance which again affects the wake. The local wind speed is also affected by the presence of upstream WECS and the presence of any other flow obstacles, as well as the terrain topography.

A reliable model should therefore be able to account for all the above factors. Reliable wind flow modeling close to the ground requires the solution of governing P.D.E.s; the real challenge here is appropriate discretization of the P.D.E.s over the vast extent of the three-dimensional solution plane, for wind farms extend several kilometers in each direction. A great deal of ingenuity must be introduced in order to render the problem tractable without undue loss of accuracy.

The paper addresses the challenges one at a time offering solutions for each one. The paper also presents a new model which employs cyclic boundary conditions together with boundary fitted co-ordinates to predict the performance of very large wind farms erected on flat terrain, when the free wind is inclined to the array center-lines.

MODELLING OF LOCAL WIND FLOW

Atmospheric wind flow may be characterized by wind aloft and wind in the layer close to the ground known as the near surface flow. The wind aloft depends on many global meteorological factors ; it is best treated as a random variable when time averaged performance is being calculated. Otherwise, it is introduced as an imposed boundary condition in the mathematical model for the near surface flow. The same treatment applies to the wind far upstream and downstream of the wind farm. The height of the constant stress, near surface layer depends on many factors , but it may safely be assumed that the entire WECS lies within this layer, and that the effect of the WECS on the atmospheric flow is also confined to this layer. Thus the integration domain employed to predict the local wind flow is restricted to a limited region encompassing the wind farm and of a vertical distance high enough to include all the interference effects of the WECS, but lying entirely within the constant stress layer.

The flow within this layer is fully turbulent and hence requires an appropriate turbulence model for its prediction. Many models exist in the literature which have been applied to predict the flow in the atmospheric surface layer, with varying degrees of success. The models themselves vary widely in sophistication; the more sophisticated the model the more demanding the computational effort. With present day computers, a balance between accuracy and requirements for the problem considered seems to point towards two equation models of turbulence. The (k-ε) model of turbulence [1] is recommended here since it is has been tested successfully for many boundary layer flows, including atmospheric surface layer flows under both neutrally stable conditions, and stratified conditions, [2,3,4].

Such a mathematical model was previously presented for wind-farms with wind blowing normal to the turbine rows[5]; some of its features are described here for sake of completeness. The model comprises three dimensional differential equations expressing the conservation of mass, balance of momentum, and transport of the kinetic energy of turbulence , k and its rate of dissipation,ε, according to the (k-ε) model of turbulence. Employing the Cartesian system of coordinates(x,y,z) the governing equations may all be cast in the following concise form:

$$\nabla . (\rho \underline{V} \phi) = \nabla . (\Gamma_\phi \nabla\phi) + S_\phi \qquad (1)$$

where $\nabla \equiv \partial/\partial x\ \underline{i} + \partial/\partial y\ \underline{j} + \partial/\partial z\ \underline{k}$ is the Nabla operator, ϕ denotes any dependent variable , $\underline{V} = u\ \underline{i} + v\ \underline{j} + w\ \underline{k}$ is the velocity vector, Γ_ϕ and S_ϕ are the diffusion coefficient and source term, respectively , for the variable ϕ . The mass conservation equation may also be expressed in the form of Eq.(1) with $\phi \equiv 1$ and $\Gamma_\phi = S_\phi = 0$. For the velocity components $\Gamma_\phi = \mu_e$, whereas $\Gamma_k = \mu_t/\sigma_k$ and $\Gamma_\varepsilon = \mu_t/\sigma_\varepsilon$; the S_ϕ expressions are presented in Table.1, where p denotes the static pressure .

Table.1 Source term expressions

ϕ	S_ϕ
u	$-\partial p/\partial x+\partial(\mu_e\partial u/\partial x)/\partial x+\partial(\mu_e\partial v/\partial x)/\partial y+\partial(\mu_e\partial w/\partial x)/\partial z$
v	$-\partial p/\partial y+\partial(\mu_e\partial u/\partial y)/\partial x+\partial(\mu_e\partial v/\partial y)/\partial y+\partial(\mu_e\partial w/\partial y)/\partial z$
w	$-\partial p/\partial z+\partial(\mu_e\partial u/\partial z)/\partial x+\partial(\mu_e\partial v/\partial z)/\partial y+\partial(\mu_e\partial w/\partial z)/\partial z$
k	$G_k^* - \rho\ \varepsilon$
ε	$C_1\ \varepsilon/k.G_k^* - C_2\ \rho\ \varepsilon^2/k$
$^*G_k = \mu_t \{2[(\partial u/\partial x)^2 + (\partial v/\partial y)^2 + (\partial w/\partial z)^2] + (\partial u/\partial y+\partial v/\partial x)^2 + (\partial u/\partial z+\partial w/\partial x)^2 + (\partial v/\partial z+\partial w/\partial y)^2 \}$, $\mu_t \equiv \rho\ C_\mu\ k^2/\varepsilon$	

The effective viscosity $\mu_e = \mu + \mu_t$, where μ is the molecular viscosity , and μ_t is the eddy diffusivity. The turbulence model constants $C_1, C_2, C_\mu, \sigma_k$ and σ_ε are presented in Table.2.

Table.2. Turbulence model constants

C_1	C_2	C_μ	σ_k	σ_ε
1.44	1.92	.09	1.0	1.3

Boundary Conditions : Aligning the z-direction with the direction of the wind aloft, and the y-direction with the vertical upwards, the following boundary conditions are applied:

a) **Inflow boundary** (z=0):

This is assumed to be a fully developed, neutrally stable atmospheric flow boundary, hence:

$$u = v = 0 \quad (2.a)$$
$$w = 1 / \kappa . (\tau_s/\rho)^{1/2} \ln(y/y_o) \quad (2.b)$$

where τ_s is the shear stress at the ground surface and y_o is its aerodynamic roughness. Available charts [6]may be employed to specify y_o for any terrain type, after which τ_s may be calculated for a given value of w at a given height y; alternatively measurements of w at two different heights at the same locations may be employed to determine y_o and τ_s.

$$k = \tau_s/(\rho C_\mu^{1/2}) \quad (2.c)$$
$$\varepsilon = (\tau_s/\rho)^{3/2} / \kappa y \quad (2.d)$$

b) **Outflow boundary** ($z=z_{max}$)

This boundary is taken far enough downstream of the turbines for the flow there to be practically fully developed; hence a uniform exit pressure is specified over the whole exit plane and z-direction gradients are assumed to be absent for all dependent variables except w.

c) **Top boundary** ($y=y_{max}$)

The height y_{max} is taken great enough that the flow there may be assumed to conform to free atmospheric flow; hence the dependent variable values are generally calculated from Eqs.(2) with $y = y_{max}$. However, in order to allow for weak inflows and outflows across this boundary resulting from possible variations in ground topography and/or effects of flow obstructions near the ground, v has been floated at this boundary and a uniform pressure is assumed aloft.

d) **Ground boundary** (y = 0)

Wall functions are employed at this boundary to connect the values at the near boundary internal nodes to those at the boundary itself, thus :

$$u_s = v_s = w_s = 0 \quad (3.a)$$
$$\tau_s = \rho [\kappa/\ln(y/y_o)]^2 (w^2 + u^2) \quad (3.b)$$
$$k = \tau_s/(\rho C_\mu^{1/2}) \quad (3.c)$$
$$\varepsilon = (\tau_s/\rho)^{3/2} / \kappa y \quad (3.d)$$

where the subscript "s" denotes surface values, the other values being evaluated at the near surface grid node. The values of k and ε are fixed at these nodes according to Eqs.(3c,d), respectively.

e) **Side boundaries** ($x = 0$ & $x= x_{max}$)

. If the wind is blowing normal to the row of WECS, symmetry boundary conditions may be imposed at both boundaries, with the exception of the edge turbines were free wind boundary conditions may be imposed.

SOLUTION PROCEDURE

A finite-volume method is employed here to discretize the governing equations[7], which employs a solution procedure derived from the SIMPLE algorithm[8]. The result of the discretization of the differential equations is an algebraic equation at each control volume of the general form :

$$\phi_p = (\Sigma A_j \phi_j + S_{\phi,e})/(\Sigma A_j + S_{\phi,i}) \quad (4)$$

where ϕ_p denotes the value of ϕ at the considered node "p", A_j is a coefficient expressing the sum of the convection and diffusion contributions at the control volume surface "j", and the summation is performed over all six control volume surfaces. $S_{\phi,e}$ and $S_{\phi,i}$ denote the explicit and implicit components, respectively , of the source term S_ϕ. Thus the total source term acting on the control volume is effectively :

$$S_\phi = S_{\phi,e} - S_{\phi,i} \phi_p \quad (5)$$

The conditions at the boundaries of the solution domain are all introduced through the source terms of Eq.(4). The wind turbine effect on the flow is also introduced through additional source terms.

HAWT CHARACTERISTICS & 2 WAY COUPLING

The turbine characteristics are required in the form of axial thrust T, and output power P, as a function of the local flow velocity *at the turbine rotor face,* w_T. They may be derived from either direct measurements or mathematical modeling, e.g. employing blade element theory [9]. Alternatively, If, as often the case, the dependent variables are already provided as a function of the undisturbed free stream velocity, then actuator disc theory may be employed to convert it to the desired form. Details of this model were presented in [10].

The T-w_T characteristic of the turbine is first linearized in the range employed , and presented in the form of Eq.(5) to the source terms of the w-momentum equations in the rotor plane . Since for wind turbine characteristics, T increases with w_T , the coefficient $S_{\phi,i}$ is positive and hence increases the diagonal dominance of the matrix of coefficients of the finite volume equations; this has a positive effect on the convergence rate of the iterative solution.

It is assumed that the turbines will influence the atmospheric flow primarily by way of pressure rise at the rotor disk which counteracts the rotor thrust, and to a lesser extent by the introduction of angular momentum downstream the rotor caused by rotor twirl. In addition, the tower, hub and nacelle introduce resistance and obstruction to the near flow field, and their influence is also included. Details of simulating twirl, tower, hub and nacelle obstruction, terrain irregularity and ground obstructions were all presented together with other details in [10] for a single wind turbine; the implementation for the individual turbines of a wind farm is no different

WIND AT AN ANGLE

Almost all reported predictions on wind farm interference effects concentrate on wind flow in the predominant wind direction, i.e. the case were wind flows normal to the turbine row-lines, and alternate rows of WECS present aligned units. Apart from the importance of this case, it is by far the simplest to compute; for it allows relatively small integration domains to be considered, which display symmetry and other simple boundary conditions. Moreover, Cartesian co-ordinates may readily be adopted.

However, wind does blow from more than one direction and it is important to predict the wind farm performance for all directions. To achieve this economically requires much ingenuity, for example exploiting all terrain features to introduce justifiable boundaries and present acceptable assumptions. Alternatively, the wind-farm may be divided into areas of manageable proportions with some overlap and conveying the effects of one region to another; in some instances the effects may be assumed to propagate in one direction by virtue of dominant up-wind influences. Each case would have to be treated individually.

For wind-farms located on flat open terrain, such as the ones erected in Zafarana, Egypt, a model is presented here for the first time which is economical, regardless of the farm size, as long as an orderly array of identical WECS units are employed. The model exploits the typical staggered, but orderly structure of wind farm arrays. To do so, it requires the use of non-orthogonal boundary fitted co-ordinates together with cyclic boundary conditions.

The mathematical model employs the same governing equations presented earlier, eqns(1), but cast in BFC [11]. The boundary conditions at inlet to the domain, outlet and ground are the same as those presented in eqns(2-3). A constant pressure boundary condition is employed at the top boundary which is horizontal. However, cyclic boundary conditions, e.g.[12] are introduced at the side boundaries.

The particular features of the model are best described by an example which comprises a wind farm with 5 rows of turbines across the predominant wind direction and an infinite number of equally spaced turbines along each turbine row. The WECS have the same characteristics employed in [6], and 7 diameter spacing is retained between successive turbine rows in the pre-dominant wind direction, while 5 diameter spacing is retained between adjacent turbines in the cross-stream direction, i.e. along the turbine rows. The free atmospheric wind blows at a 45^{o} angle with the row-lines.

The horizontal cross-section of the integration domain is a rhombus, Figure 1, whose shorter side is normal to the predominant wind direction and therefore parallel to one of the turbine row-lines; its direction will be referred to here as the

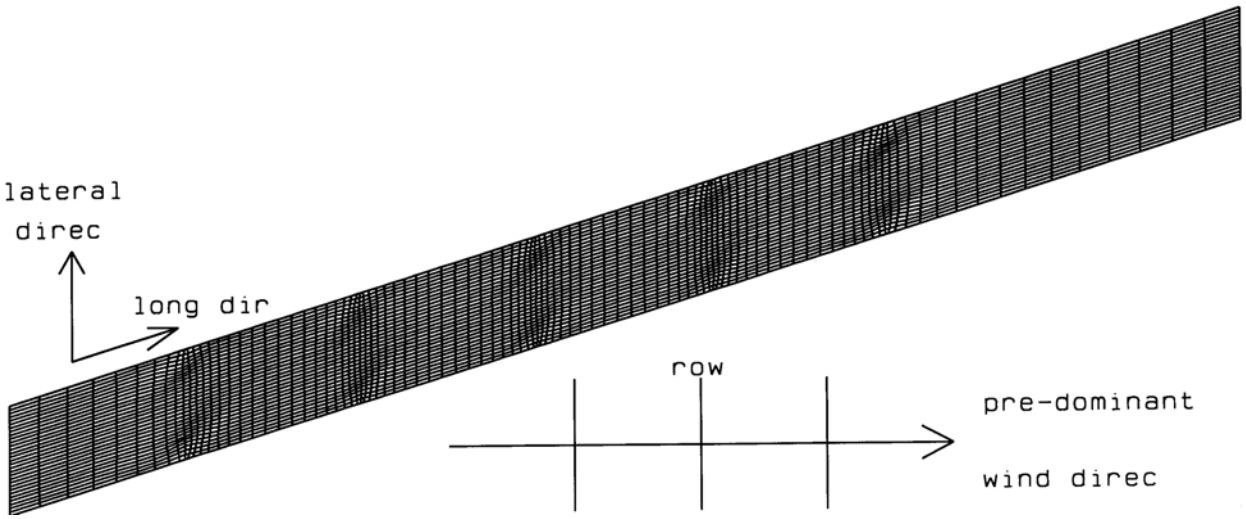

Figure 1. Grid distribution in horizontal plane adjacent to ground

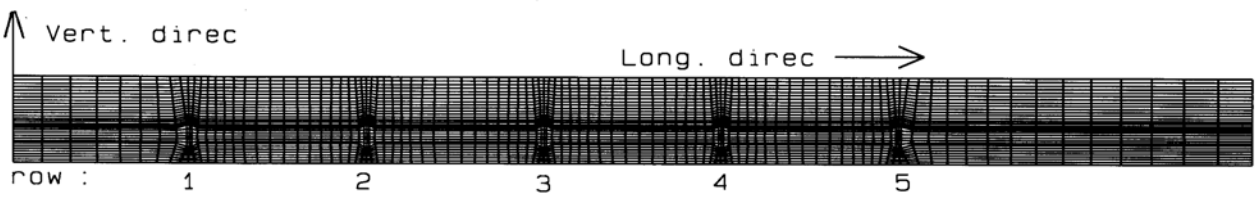

Figure 2. Grid distribution in vertical plane passing through WECS center lines.

lateral direction. The longer side is parallel to the line connecting the closest successive staggered turbine center-lines. The latter is a straight line provided the array is ordered with equal spacing in each direction; its direction will be referred to as the longitudinal direction. The length of the shorter side is equal to the lateral distance between adjacent turbine units. The longer sides protrude sufficiently outwards in the upstream and downstream directions that free wind conditions, and uniform exit pressure conditions may be applied, respectively. Figure 1 displays the BFC grid in a horizontal surface adjacent to the ground; 100 control volumes are employed in the longitudinal direction, and 30 control volumes are employed in the lateral direction.

By imposing cyclic boundary conditions, along the longitudinal vertical boundaries, the flow over this relatively minute slab of the wind farm represents the flow over almost all of the wind-farm, with the small exception of the lateral edges of the wind-farm. The effect of the latter on performance may usually be neglected, else separate integration domains with free wind boundary conditions would need to be employed close to the edges.

Figure 2 displays the grid distribution in a vertical surface passing through the turbine center-lines. The grid spacing is seen to be refined near the location of the turbine row-lines, which are numbered consecutively from 1 to 5.

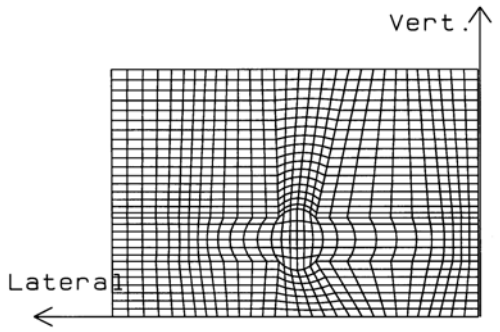

Figure 3. Grid in vertical surface passing through rotor.

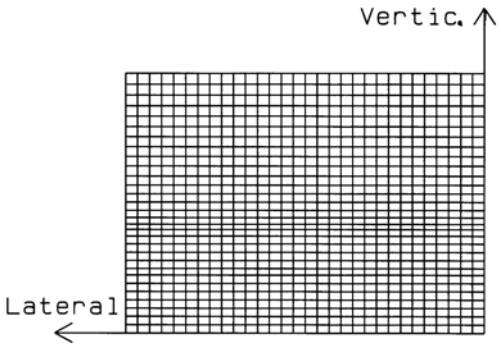

Figure 4. Grid in vertical surface at exit plane.

Figure 3 shows the grid distribution in a vertical surface encompassing one of the turbine-rotors; the display is a projection of the grid on a vertical-lateral directions plane. Some of the grid lines are seen to outline an elliptic shape; this is the projection of the circular rotor on the projection plane, the rotor of course being aligned normal to the incoming wind direction. Figure 4 displays the same grid distribution at the far downstream plane; here the grid surface lies on the projection plane itself, and the grid is rectangular since there are no turbine rotors to outline. Intermediate computational surfaces display grid distributions which develop gradually from one grid shape to the other.

Figure 5 displays part of the BFC grid in a horizontal plane passing through the center-lines of the wind-turbine rotors, centered around a third row turbine. It is noticed that three straight , parallel grid lines appear at longitudinal locations halfway across the integration domain. The middle one corresponds to the location of the wind turbine rotor and is seen to be normal to the free wind direction, as should be. The immediate upstream and downstream grid lines comprise identical but shifted parallel discs. This trick facilitates tremendously the expression of the WECS characteristics and increases accuracy, since it ensures that the velocity component passing through the rotor plane is normal to that plane , while the other components are parallel to it. Hence resolution of velocity components and their source terms is eliminated altogether.

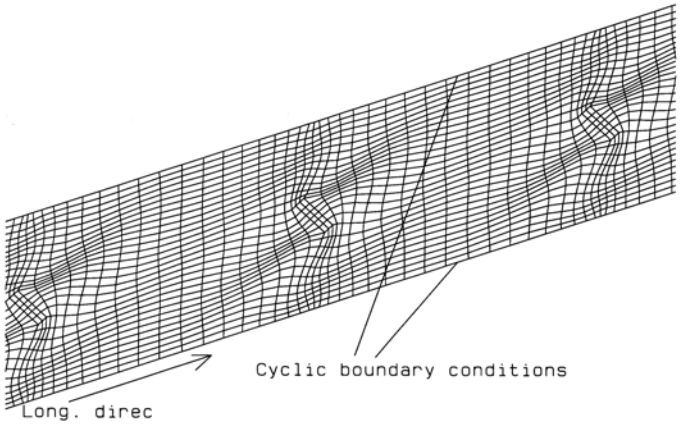

Figure 5. Grid distribution in rotor c.l. horizontal plane

Figure 5 also discloses that a useful outcome of selecting the longitudinal direction to correspond to the line connecting the successive turbine axis is that all turbines have the same coordinates in the lateral and vertical directions, differing only in the longitudinal coordinate. This has the advantage of facilitating the design of the BFC grid and the expression of turbine boundary conditions. Moreover, the grid distribution shows that although the distribution is non-uniform, identical grid spacing is introduced along the side boundaries ; this is

necessary for proper specification of cyclic boundary-conditions.

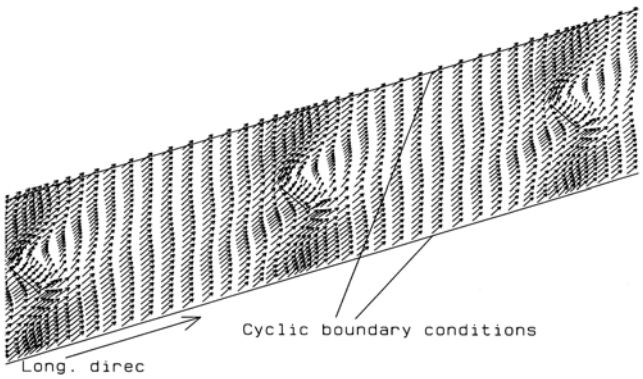

Figure 6. Velocity vectors in rotor c.l. horizontal surface.

Figure 6 displays the predicted velocity vectors in a semi-horizontal surface passing through the wind-turbines centerlines. It is seen that wind crosses the side boundaries but that the velocity vectors repeat themselves over the side boundaries, due to the cyclic boundary conditions.

Figure 7 displays an enlargement of Figure 6, centered over the third turbine. The velocity vectors clearly display the wake generated immediately downstream the wind turbine rotor. plane.

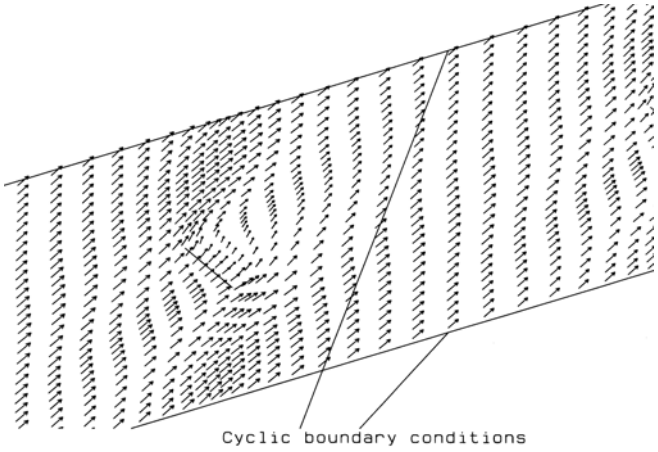

Figure 7. Enlargement of velocity vectors around third turbine.

Figure 8 displays the corresponding pressure contour lines. A total of 100 equal interval contour-lines are employed which cover the whole predicted pressure range in the plane considered. Thus, the contour lines are very tightly packed in the neighborhood of the turbine rotor, where large pressure gradients appear; to an extent that they appear as one solid block. Elsewhere, the pressure gradients are much less severe.

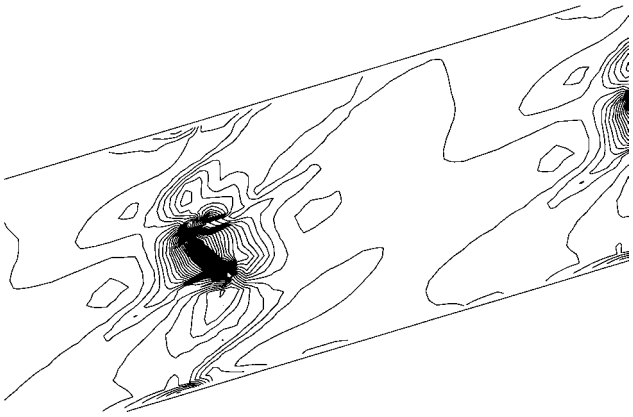

Figure 8. Pressure contour lines in horizontal plane

Figure 9 displays the predicted velocity vectors in part of the vertical surface passing through the turbine-rotors centerlines. The vectors display an obvious wake effect downstream the turbine rotors, which is compatible with Figures 6 and 7. They also reveal that the momentum deficiency in the wake is rapidly replenished before reaching the second row of turbines, although very careful observation and numerical printouts show that the recovery is not 100%. This is what causes the wake interference losses.

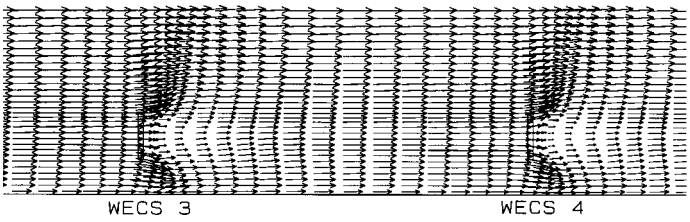

Figure 9. Velocity vectors in vertical plane

Figure 10 reveals the velocity vectors in a vertical surface encompassing the turbine rotor of WECS No.2, together with an outline of the rotor; the vectors are projected over a vertical-lateral direction plane, hence the elliptic shape of the rotor. The vectors display a divergence of wind flow as it flow through the rotor, which is compatible with the wake effect displayed in the other vector diagrams .

Figure 10 also shows that the velocity vectors at the top plane are practically horizontal, indicating that the vertical extent of the integration domain is sufficiently large for the constant pressure boundary conditions to be applicable. It is noted that the vertical plane displayed here is the one incorporating the rotor, and hence the one displaying maximum obstruction to the wind flow and therefore maximum vertical motion.

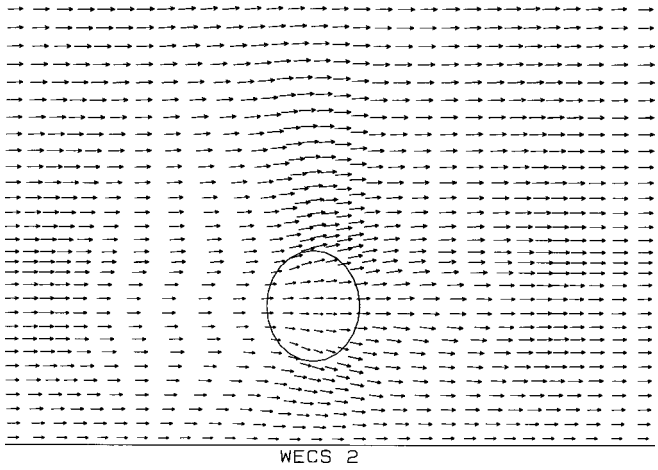

Figure 10. Vectors on the rotor surface.

STATISTICALLY AVERAGED PERFORMANCE

The previous sections presented means of predicting the performance of a wind farm for a given free wind speed and direction aloft. Because these quantities are constantly fluctuating, what interests engineers is the time average performance, i.e. average power output . This requires the knowledge of the wind speed frequency distribution in all of the 360^o horizontal directions. In practice, it is sufficient to know the frequency of the wind speed lying in discrete intervals in 45^0 segments, e.g. the N,NE,E,..NW directions. The more the intervals the better.

For each wind direction, the power generated by the farm at the average wind-speed in the speed-interval is predicted as described earlier, and multiplied by the frequency of that interval (proportion of time wind-peed in the given direction lies in that speed-interval). Summation of the product of the power generated at a certain wind-speed multiplied by frequency of the speed-interval yields the average power generated by the wind blowing in that direction. Summation of the product of the average power generated in any one direction multiplied by frequency of wind blowing in that direction, yields the average power generated by the wind farm. If the frequencies express proportion of time over a particular month then the average represents a monthly average, if they express proportion of time over a year then the average is an annual average.

How are the frequencies determined? the answer is field measurements, possibly with some imperical relations to bridge the gap. For example, the Weibull distribution may be employed to predict the frequency distribution over a large number of intervals; the Weibull parameters would be calculated from the measured frequency distributions over a limited number of intervals, as demonstrated in [13]. In the limiting case of only the mean wind speed being reported for each direction, i.e. a simple wind-rose, the wind-speed frequency distribution for that direction may be calculated employing the Rayleigh distribution; albeit with less accuracy.

SUMMARY & CONCLUSIONS

The paper discusses the problems associated with the computation of large wind-farm performance. It then describes a practical modeling approach for computation of this performance.

One of the important contributions of this paper is the presentation and application of a model for the prediction of wind farm performance when wind blows at an arbitrary angle, employing cyclic boundary conditions and boundary fitted coordinates. To the best of the authors knowledge, it is presented here for the first time.

REFERENCES

1. Launder,B.E. and Spalding,D.B.,1974 - "The Numerical Computation of Turbulent Flows", J. Computer Methods in Applied Mechanics and Eng., Vol.3, pp. 269-289.
2. Burman,J., 1995 - "Simulation of the Boundary Layer in a Neutrally Stratified Atmosphere Using Phoenics", Phoenics J. of CFD and its Applications, Vol.8, No.2, pp. 105-138.
3. Grundberg,S. , 1994 - "Simulation of the Surface Layer of Stratified Atmosphere Using Phoenics", Phoenics J.of CFD and its Applications, Vol.7., No.1, pp. 8-33.
4. Abou-Arab,T.W. and Serag-Eldin,M.A.,1992, "Turbulence Modeling and Simulation of Atmospheric Boundary Layers", ASME J. of Fluids Engineering, Vol.114, No.1, pp.40-44.
5. Serag-Eldin,,M.A.1999, - "Prediction of Interference Effects in a Wind Farm". Proceedings of 3rd ASME/JSME Joint Fluids Engineering Conference, July 18-23, San Francisco, California, paper No.FEDSM99-7051.
6. Cermak,J.E., 1975 - "Applications of Fluid Mechanics to Wind Engineering-Freeman Scholar Lecture" , ASME J. Fluids Engineering, Vol.97, pp. 9-38.
7. Patankar,S.V.,1980 - "Numerical Heat Transfer and Fluid Flow", Hemisphere publishers, London and N.Y.
8. Carreto,L.S.,Gosman,A.D., Patankar,S.V.,& Spalding,D.B., 1973 - "Two Calculation Procedures for Steady Three-Dimensional Flow with Recirculation" , Proc. 3rd Int. Conf. Num. Methods in Fluid Mechs., Vol II, pp.60-98.
9. Eggleston,D.M., and Stoddard,F.S, 1987 - "Wind Turbine Engineering Design" , Van Nostrand Reinhold Company, N.Y..

10. Serag-Eldin,M.A.,1997 - "Prediction of the Atmospheric Flow Near a HAWT", Proc. of the Numerical Methods in Thermal Problems Conf.,R.W.Lewis et al.,(eds)., Pineridge Press, Swansea, U.K., Vol.X., pp970-981.
11. Hedberg,P.K. , Rosten,H.I. and Spalding,D.B.,1986 - "The PHOENICS Equations", CHAM Report TR/99, October.
12. Serag-Eldin,M.A. and Spalding,D.B., 1981,"A Computational Procedure for Three-Dimensional Recirculating Flows Inside Can Combustors", Numerical Methods in Heat Transfer, R.Lewis,K.Morgan and O.C.Zienkiewicz, (eds),John-Wiley & Sons, N.Y., pp.445-466.
13. Koeppl,G.W., 1982 - Putnam's Power from the Wind, Van Nostrand Reinhold Company, pp.241-247.